International Journal of Pharmaceutics 477 (2014) 113–121

Contents lists available at ScienceDirect

International Journal of Pharmaceutics

journal homepage: www.elsevier.com/locate/ijpharm

Pharmaceutical nanotechnology

Antibacterial properties of laser spinning glass nanofibers

M.M. Echezarreta-López [a,*], T. De Miguel [b], F. Quintero [c], J. Pou [c], M. Landin [a]

[a] Departamento de Farmacia y Tecnología Farmacéutica, Facultad de Farmacia, Campus Vida, Universidad Santiago de Compostela, Santiago de Compostela 15782, Spain
[b] Departamento de Microbiología y Parasitología, Facultad de Farmacia, Campus Vida, Universidad Santiago de Compostela, Santiago de Compostela 15782, Spain
[c] Departamento de Física Aplicada, EE Industrial, Universidad de Vigo, 36310, Spain

ARTICLE INFO

Article history:
Received 23 June 2014
Received in revised form 23 September 2014
Accepted 26 September 2014
Available online 13 October 2014

Keywords:
Bioactive glasses
Bioinert glasses
Biocompatibility
Antibacterial properties
Nanofibers
Laser spinning
Dynamic conditions

ABSTRACT

A laser-spinning technique has been used to produce amorphous, dense and flexible glass nanofibers of two different compositions with potential utility as reinforcement materials in composites, fillers in bone defects or scaffolds (3D structures) for tissue engineering. Morphological and microstructural analyses have been carried out using SEM–EDX, ATR-FTIR and TEM. Bioactivity studies allow the nanofibers with high proportion in SiO_2 (S18/12) to be classified as a bioinert glass and the nanofibers with high proportion of calcium (ICIE16) as a bioactive glass. The cell viability tests (MTT) show high biocompatibility of the laser spinning glass nanofibers. Results from the antibacterial activity study carried out using dynamic conditions revealed that the bioactive glass nanofibers show a dose-dependent bactericidal effect on *Sthaphylococcus aureus* (*S. aureus*) while the bioinert glass nanofibers show a bacteriostatic effect also dose-dependent. The antibacterial activity has been related to the release of alkaline ions, the increase of pH of the medium and also the formation of needle-like aggregates of calcium phosphate at the surface of the bioactive glass nanofibers which act as a physical mechanism against bacteria.

The antibacterial properties give an additional value to the laser-spinning glass nanofibers for different biomedical applications, such as treating or preventing surgery-associated infections.

1. Introduction

Bioactive glasses (BGs) are inorganic materials with interesting properties in biomedicine (Kokubo, 2008). Applications in the areas of orthopedics, dentistry or tissue regeneration have been developed on the basis of their ability to react in the presence of biological fluids leading bioactive intermediate stages and favoring the formation of new tissues (Hench and Wilson, 1993). An interesting property in the biomedical field, which has been described for some bioactive glasses, is the capacity of inhibiting growth or even killing different bacteria (Stoor et al., 1998; Munukka et al., 2008). There is a wide range of literature analysing the effect of the composition, particle size or morphology of the bioactive glasses on their antibacterial activity. However, the great variability of conditions used to perform the studies (e.g., bacteria studied, microbiological conditions, glass composition and morphology, etc.) hinders the specific factors influencing bactericidal capacity to be determined. In a previous paper, we have collected historical data and analysed them by a process named data mining using an artificial intelligence technique (neurofuzzy logic) (Echezarreta-López and Landin, 2013). Our results allowed us to conclude that the antibacterial activity is mainly determined by SiO_2 content, the release of alkaline ions to the medium and the increase of pH of the medium.

In the last few decades many researchers have established several methods to obtain improved bioactive glasses (Jones, 2013). The long term benefits of nanofeatures in those fields have been pointed out by different authors. Sato and Webster have shown the importance of nanostructures in orthopedic applications, suggesting that nanophase materials promote new bone formation due to the similarity with the nanometric dimensions of the bone tissue components (Sato and Webster, 2004). Biomaterial–biological interactions are related to modifications in the surface at nanometric level with important consequences in their applicability in tissue regeneration (Khang et al., 2010; Chiara et al., 2012) or dental integration (Bressan et al., 2013). Quintero et al. have developed a novel technique of producing glass fibers of nanometric diameters with specific and controllable chemical compositions using a laser spinning procedure. The developed technique allows the rapid

* Corresponding author. Tel.: +34881815252; fax: +34881815038.
E-mail address: mmagdalena.echezarreta@usc.es (M.M. Echezarreta-López).

http://dx.doi.org/10.1016/j.ijpharm.2014.09.050
0378-5173/

production of dense glass nanofibers that can be used as bioactive reinforcement materials in composites, fillers in bone defects or scaffolds (3D structures) for tissue engineering (Quintero et al., 2009a).

On this basis, the aim of this study is to evaluate, for the first time, the potential antibacterial properties of the nanofibers of different compositions produced by the laser spinning technique. The two materials studied include, a high silicon content glass nanofibers (S18/12) and a high calcium content glass nanofibers (ICIE16). The significant variations in their composition make their dissolution process extremely different, which may have a potential effect on their antibacterial properties. Structural and surface modifications of nanofibers (SEM–EDX, ATR-FTIR and TEM) analysed before and after microbiological studies in dynamic conditions should allow the antibacterial activity to be explained.

2. Materials and methods

2.1. Glass nanofibers preparation

Glass nanofibers were obtained by a laser spinning technique as previously described by Quintero et al. (2009a). First, a blend of raw materials including soda, lime, silica and phosphorous oxide, were melted in a platinum crucible at 1500 °C and poured into a graphite mold to obtain flat plates with thickness of 5 mm and the desired compositions. The composition of these glass plates was analysed by X-ray fluorescence (XRF) obtaining the values included in Table 1. These glass plates were then employed as the precursor material for the laser spinning process. A high power CO_2 laser (Rofin Sinar DC 035) emitting, in continuous mode, a beam of infrared radiation with wavelength of 10.6 μm was focused over the glass plates to set irradiance to 1×10^5 W/cm^2 and advance speed of 10 mm/s. The assist gas employed was compressed air at 12 bar. The high speed gas jet is responsible for the extremely quick elongation and cooling of a small volume of the molten viscous material, thus high form factor fibers are formed.

Laser-spinning glasses nanofibers, as supplied, were immersed in Milli-Q water for 1 min without stirring, filtered through an acetate cellulose membrane (0.45 μm) and dried at 50 °C for 24 h.

2.2. Characterization studies

Some structural and morphological characteristics of glass nanofibers were analysed. Attenuated total reflectance-infrared spectroscopy (ATR-FTIR) analyses were performed on a 670IR Varian (USA) spectrometer equipped with a Gladi-ATR (Pike, USA). The spectra were recorded on an average of 256 scans at a resolution of 4 cm^{-1} in the 400–4000 cm^{-1} range. The glass nanofibers were analysed by FTIR before and after the antibacterial properties studies were carried out.

The surface morphology and composition modifications of glass nanofibers and bacteria were observed by scanning electron microscopy (SEM) (Leo 435VP, Cambridge, UK) with X-ray energy dispersive spectroscopy microanalysis (EDX, Oxford 300). The samples were coated with gold to eliminate charging effects. Transmission electron microscopy (TEM) (JEOL JEM-1011, Tokyo, Japan), according to Santhana Raj et al. (2007), were employed to evaluate physical action of the glass nanofibers on the bacteria.

Table 1
Laser spinning glass nanofibers composition (mol%).

Name	SiO_2	CaO	Na_2O	K_2O	P_2O_5	MgO
ICIE16	49.46	36.27	6.60	6.60	1.07	–
S18/12	71.1	9.3	12.3	0.3	–	6.4

2.3. Bioactivity studies

Bioactivity *in vitro* tests of individual samples of ICIE16 and S18/12 nanofibers were carried out by studying their dissolution process in simulated body fluid (SBF) for 5 days. The SBF solution was prepared using the standard procedure described by Kokubo et al. (1990). Six milligrams of each nanofiber was soaked in 25 mL of SBF (pH 7.35) at 37 °C. At pre-set times of 3, 6, 12, 24, 48 and 120 h, the nanofibers were washed and dried in air. Bioactivity was related to the variations of ionic concentrations in the solution with the set time. The Ca and Si concentrations in the solution were estimated by optical emission spectroscopy inductive coupled plasma spectroscopy (ICP–OES) using a PerkinElmer Optima 3300DV system (Norwalk, USA).

2.4. Biocompatibility assay

The *in vitro* cytotoxicity tests for glass nanofibers were performed on extracts prepared by elution of the samples (75 mg/mL) in Dulbecco's modified Eagle's medium (DMEM) (GIBCOTM), supplemented with 10% fetal bovine serum (FBS) and 1% gentamicin in duplicate at 37° for 24 h and 48 h. Cell viability tests were performed with BALB/3T3 cell line (CCL 163, ATCC, USA), according to the 10993–5 protocol of the International Standardization Organization (ISO). A cell suspension of 2×10^4 cells/well in 200 μl of DMEM was added into a 96-well plate and allowed to grow. After 24 h or 48 h, different concentrations of ICIE16 and S18/12 glass nanofibers extracts (0.5, 1 and 2%) were added to the cells and the plate was incubated at 37 °C in a humidified atmosphere with 5% CO_2. A control (cells without glass nanofibers extracts) was treated in the same way. The 3-(4, 5-dimethylthiazol-2-yl)-2, 5-diphenyl tetrazolium bromide (MTT) assay was used in this study to measure cell viability. MTT assay measures intracellular mitochondrial activity of the cells, which involves reduction of MTT by intracellular dehydrogenases of viable cells to blue formazan. Cells survival was evaluated through the measurement of absorbance at 550 nm using a microplate reader (BIORAD Model 680, Hercules, CA, USA). Each experiment was carried out in duplicate.

2.5. Antibacterial properties studies

The antibacterial properties of the laser-spinning glass nanofibers were evaluated in dynamic conditions using a Gram positive bacterial strain, *Sthaphylococcus aureus* CECT 240.

S. aureus was incubated in a tryptic soy broth (TSB) medium (Oxoid, Drongen, Belgium) pH 7.3 to reach a density of about 10^6 cells/mL. Then 100 μL of this culture were inoculated into an eppendorf tube containing 900 μL of fresh TSB medium and glass nanofibers. Bacteria cultured without glass nanofibers were used as a negative control. Different concentrations (5, 25 and 75 mg/mL) of pre-washed and sterilized nanofibers were incubated for 4 days at 37 °C in an Erlenmeyer flask sealed with Parafilm® M under agitation in an orbital shaker at 200 rpm. 50 μL were taken from this culture every 24 h, 10 μL were used to check bacterial presence using SEM and the rest to perform serial dilutions. Aliquots of 50 μL of dilutions 10^{-4}, 10^{-5} and 10^{-6} were plated in triplicate on tryptic soy agar (TSA) medium and incubated at 37 °C for 24 h. After counting plate colonies, a bacterial growth index (GI) was established according to the following parameters: Level 4: >>>300 colonies (countless); Level 3: >300 colonies (countable); Level 2: 30–300 colonies; Level 1: 0–30 colonies; Level 0: no colonies.

Additionally, pH medium was measured (pH Meter GLP22 Crison, Spain) at each set time.

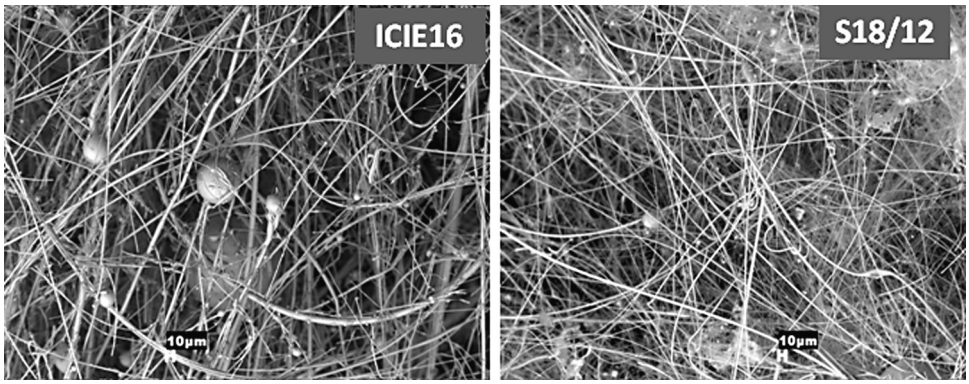

Fig. 1. SEM micrographs showing laser spinning glass nanofibers.

With the aim of analysing the structure of the remaining nanofibers, after four days culture the samples were spin-dried at 8000 rpm for 2 min (Microfuge® 22R Centrifuge Beckman Coulter™, USA). The supernatant was removed and the pellet washed twice with sterile Milli-Q water in order to ensure the removal of mineral salts from the culture medium. Afterwards, the nanofibers were evaluated by ATR-FTIR, SEM–EDX and TEM.

3. Results

3.1. Laser spinning glass nanofibers characterization

Two different compositions of glass nanofibers were obtained using the laser spinning method. SEM micrographs (Fig. 1) show an overall view of their appearance of the laser spinning nanofibers as

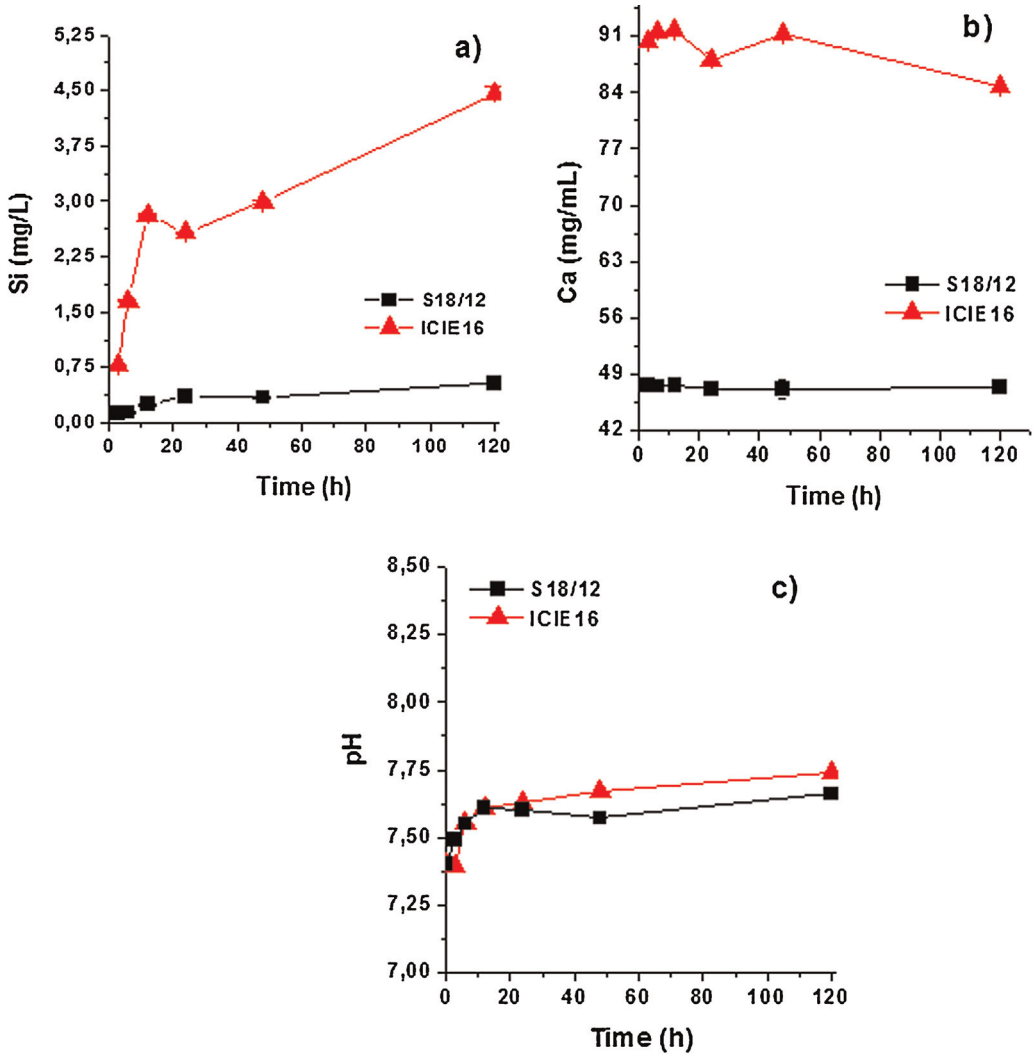

Fig. 2. Evolution of (a) silicium concentration, (b) calcium concentration and (c) pH of the medium through the bioactivity experiments by soaking laser-spinning glass nanofibers in SBF at 25 °C.

supplied. As it can be seen, they have a uniform well-defined cylindrical morphology (diameters ranging between tens of nanometers and 5 μm) and they form a disordered intertwined net where fully dense, solid and completely separated nanofibers can be observed. Some spherical particles mixed with the nanofibers can also be observed. Their formation is related to the ratio of viscosity to surface tension of the viscous filament during its elongation and cooling. At some points of the molten volume, the surface tension promotes break-up of the fluid filament into droplets, and hence, spheroidal particles are formed (Quintero et al., 2009b).

3.2. Bioactivity studies

Fig. 2 shows the cumulative variation of calcium and silicium ionic concentration and the pH of the medium during the soaking time in SBF for ICIE16 and S18/12 nanofibers. As can be observed (Fig. 2a) Si concentration in the solution continuously increases during the experiment, the increase for ICIE16 being higher than for S18/12. On the contrary, the main variation of Ca^{2+} ion concentration in SBF (Fig. 2b) occurs at the beginning of the experiment. The release of Ca^{2+} ions from the ICIE16 nanofibers is significantly higher than from S1812, corresponding to the CaO concentration in its composition. For S1812 nanofibers, the calcium concentration reaches a maximum after 12 h of soaking in SBF and did not change afterwards, while for ICIE16 nanofibers, Ca^{2+} concentration after a maximum at 12 h of the experiment show slight decreases during the following to 5 days. Variations in the ion release do not correlate with modifications in the pH as both types of nanofibers show a similar pH profile (Fig. 2c).

3.3. Biocompatibility assay

Biocompatibility of the glass nanofibers were screened using fibroblast (BALB/3T3) cell line. Fig. 3 shows the results of the cell viability percentage after incubation of cells with extracts of both S18/12 and ICIE16 glass nanofibers for 24 or 48 h. As it can be seen, the cell viability obtained is higher than 80% for both, but it is lower for the treatment with ICIE16 glass nanofibers. Results can be justified by the bioactive nature of ICIE16 glass nanofibers that promotes their fast dissolution and the release of ions in the medium.

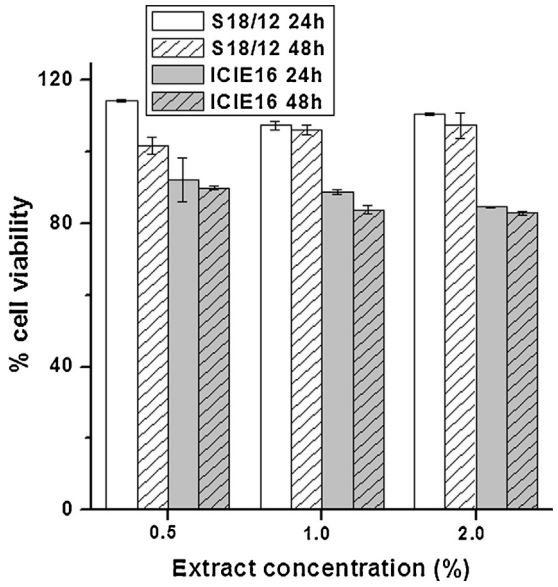

Fig. 3. Biocompatibility tests of S18/12 and ICIE16 laser spinning glass nanofibers after 24 and 48 h.

3.4. Antibacterial properties studies

The antibacterial properties of laser-spinning glass nanofibers were tested using *S. aureus* which is a Gram positive bacteria involved in an important number of infections after dental or bone implantation and this has been found to be sensitive to other bioglass materials as described by different authors (Munukka et al., 2008; Hu et al., 2009; Mortazavi et al., 2010). Fig. 4 shows the bacteria growth index profiles versus time carried out with the two varieties of nanofibers at different concentrations during the four day experiments. All the biomaterial samples have a positive effect on bacterial inhibition, however, quantitative differences can be observed with regard to the composition of the nanofiber and the concentration used for the experiment. At the highest concentration 75 mg/mL, at least a bacteriostatic effect is detected in S18/12 fibers from the beginning of the experiment. ICIE16 nanofibers show at high concentration bactericidal effect on *S. aureus*, the maximum being after 4 days when no bacteria growth is detected.

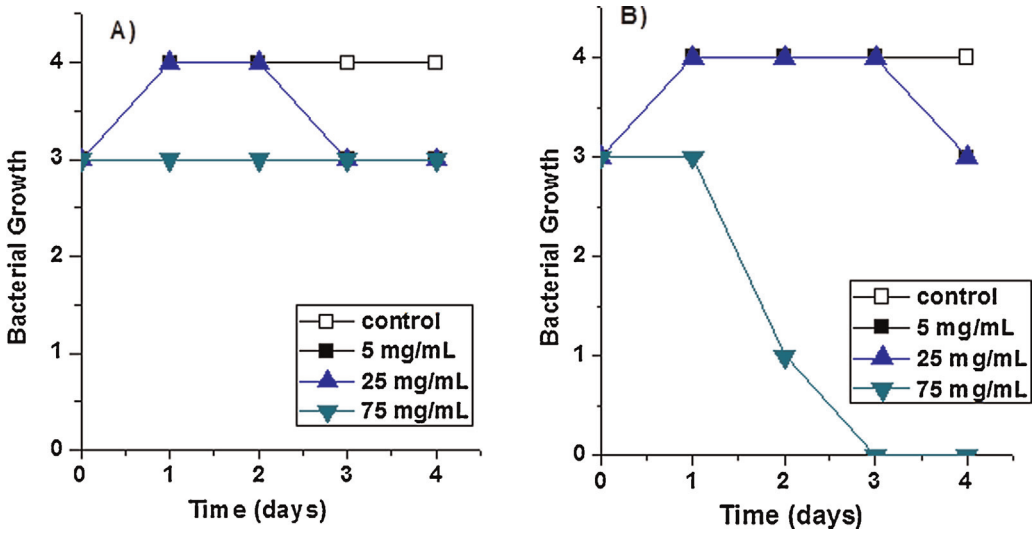

Fig. 4. Bacterial growth at different concentrations of (A) S18/12 and (B) ICIE16 laser-spinning glass nanofibers.

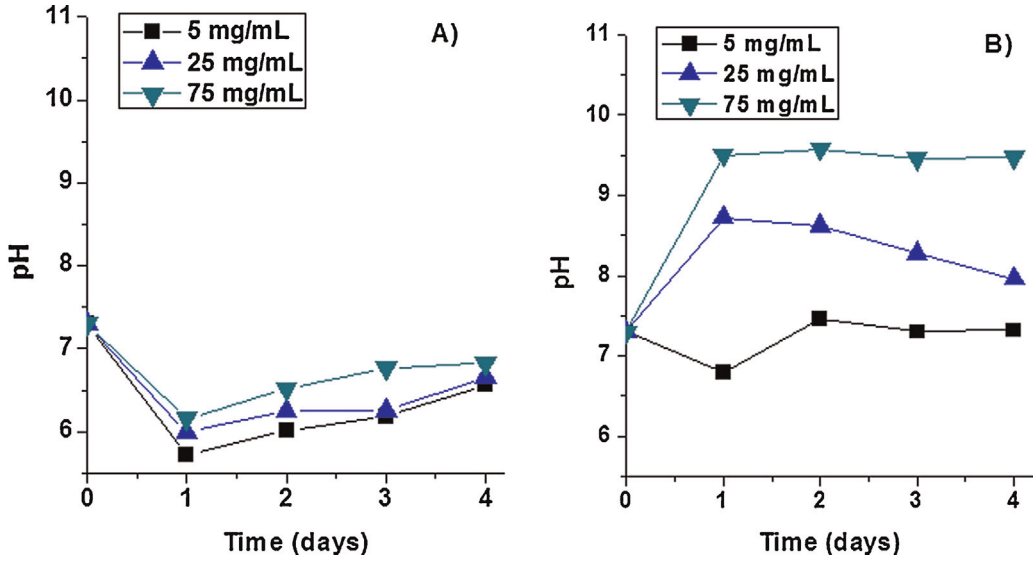

Fig. 5. Profile of pH of the medium through the microbiological studies at different concentrations of (A) S18/12 and (B) ICIE16 laser spinning glass nanofibers.

Differences in the bactericidal effect of the biomaterials can be justified by the variation in the pH of the media during the incubation period (Fig. 5). S18/12 glass nanofibers promote small variations in the pH of the medium in all the concentrations studied (pH never higher than 6.5) while ICIE16 nanofibers lead progressive increases in the pH up to values close to 9.5 when the nanofibers concentration is 75 mg/mL.

The ATR-FTIR analysis carried out on the glass nanofibers before and after the microbiological study (Fig. 6) illustrates the structural variations between nanofibers and the modifications produced as a consequence of their incubation with bacteria culture.

The main absorption bands of bioactive glasses have been described at 1024, 926 and 480 cm^{-1} and attributed to the Si—O—Si stretching mode, Si—O and Si—O—Si bend mode, respectively (Serra et al., 2003; Efimov and Pogareva, 2006). In particular, the band at 926 cm^{-1}, has been identified with the Si—O bonds of the non-bridge oxygen (NBO), a characteristic of the SiO_4 network. Those bands can also be observed in both ICIE16 and S18/12 nanofibers as supplied by the manufacturer, despite the changes generated by the incorporation of distortion ions in the network.

After 4 days incubation in the bacterial culture, strong modifications can be seen in the ATR-FTIR spectra, especially at the band at 926 cm^{-1} corresponding to NBO which is reduced in the S18/12 nanofibers and cannot be detected in the ICIE16 nanofibers. Additionally, the band at 1024 cm^{-1} shifted to 1060 cm^{-1} and a new one at 1020 cm^{-1}, which corresponds to P—O bend, appears for ICIE16 nanofibers. The formation of the hydroxyapatite (Hap) layer on the ICIE16 nanofibers after incubation in bacterial culture is also indicated by the presence of vibrational bands at 567 and 599 cm^{-1} (Saravanakumar et al., 2011). This modification cannot be observed in the S18/12 samples spectra. Those results assess important changes in the microstructure and surface of the nanofibers during the incubation experiment.

Microstructural and surface changes of ICIE16 and S18/12 nanofibers recovered from microbiological studies were deeply

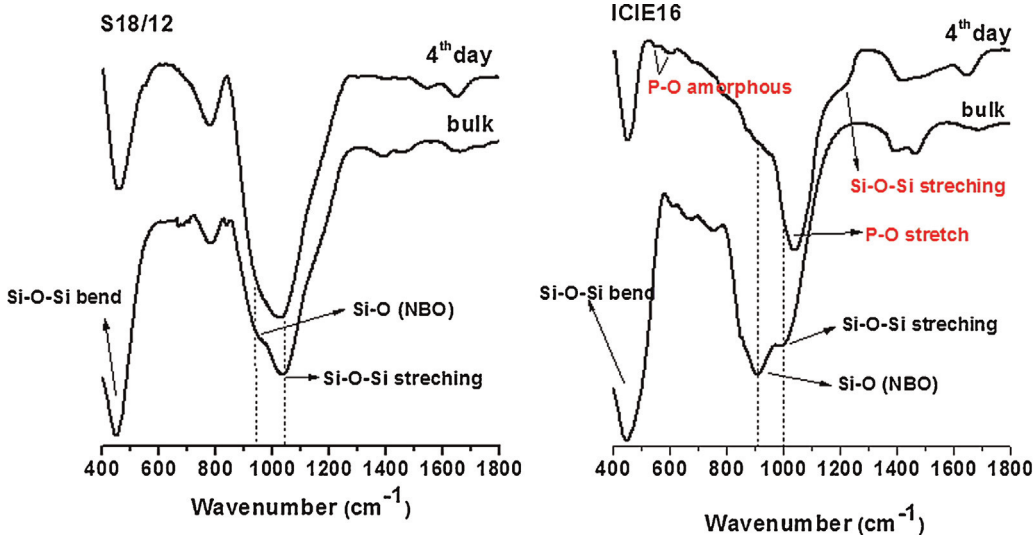

Fig. 6. Infrared spectra of glass nanofibers before and after 4 days in the presence of *S. aureus*.

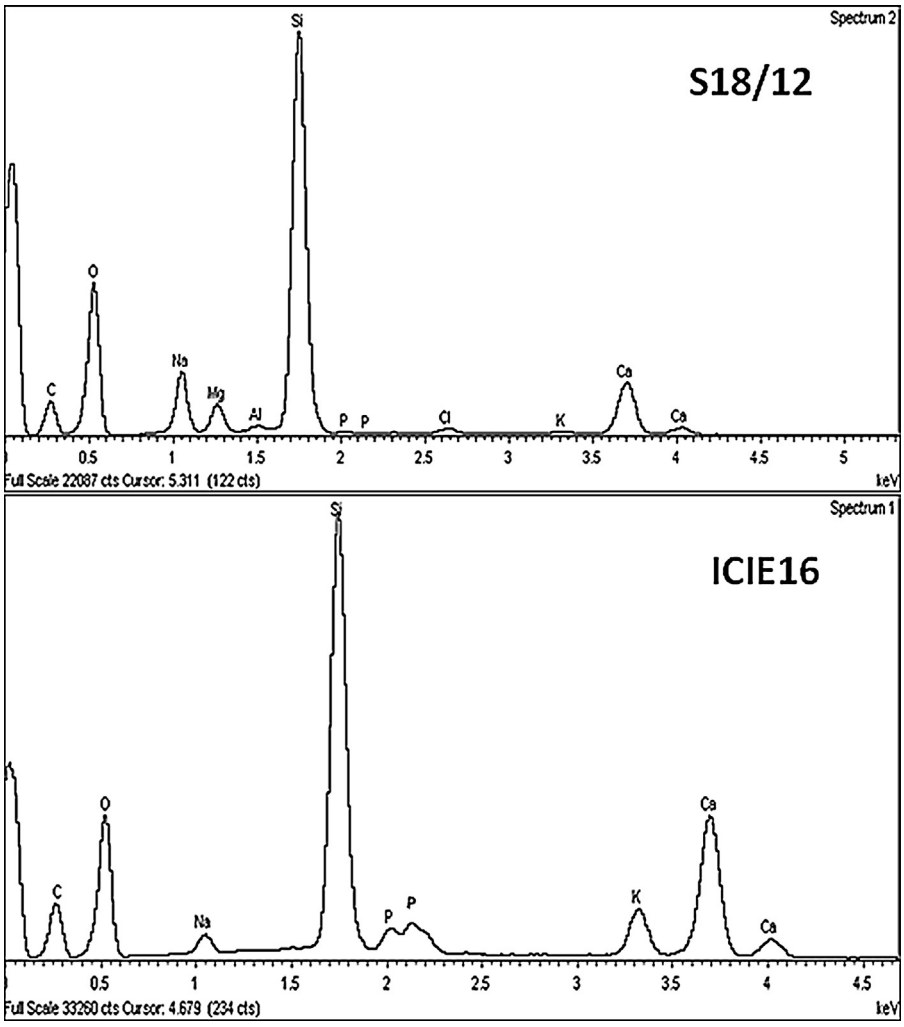

Fig. 7. SEM–EDX results for S18/12 and ICIE16 (75 mg/mL) after 4 days in the bacterial culture with stirring.

investigated by SEM coupled to EDX in order to obtain semi-quantitative information on the chemical composition of the surface of the samples. The patterns obtained for the glass nanofibers surface after 4 days in dynamic conditions (Fig. 7) is in agreement with the composition of the nanofibers as supplied. After incubation ICIE16 presents an important amount of calcium and phosphorus on the surface. The Ca/P molar ratio measured by EDX is 6.89 indicating the formation of an amorphous layer of Hap (Filgueiras et al., 1993). A thin calcium phosphate layer on the surface of ICIE16 nanofibers can be observed by SEM (Fig. 8) covering both, the remaining nanofibers and staphylococci bacteria. On the contrary, no deposition of additional layers can be observed in the S18/12 nanofibers whose surfaces appear clean without precipitates (Fig. 9).

Finally, TEM analyses results point out a physical antibacterial effect of glass nanofibers ICIE16 on bacterial structure. Fig. 10 shows numerous needle-like crystalline aggregates around the bacteria which contribute physically to their rupture and death.

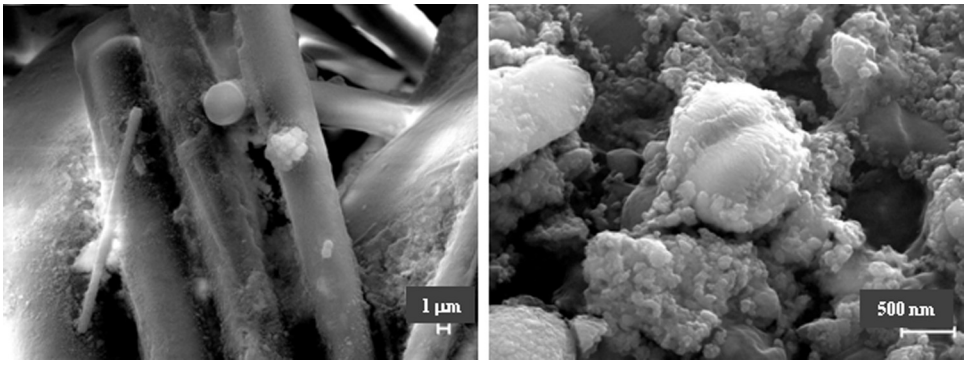

Fig. 8. SEM of ICIE16 in bacterial medium in dynamic conditions.

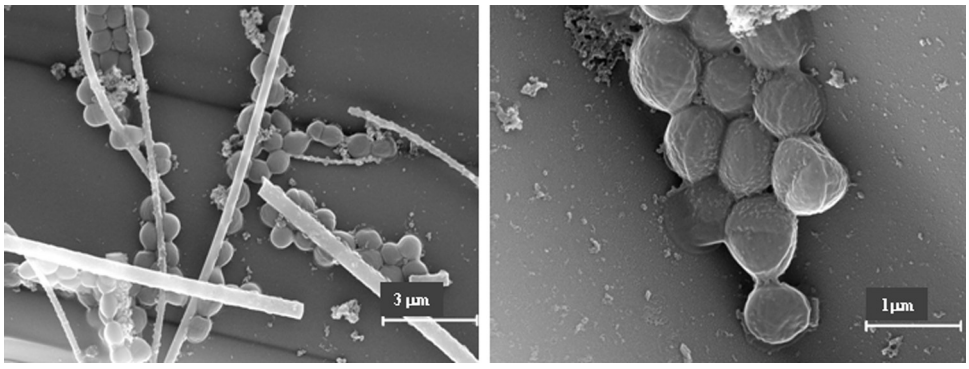

Fig. 9. SEM of S18/12 after bacterial study in dynamic conditions.

4. Discussion

The incorporation of nanomaterials in different biomedical technologies is widely known (Boccaccini et al., 2010; Bououdina et al., 2013; Parratt and Yao, 2013). In the last few years, an important number of studies on bioactive glasses (Stoor, 1998; Zhang, 2010; Mortazavi, 2010) have shown that their antibacterial activity is influenced by their composition and dissolution properties (Bellantone et al., 2000; Allan et al., 2001). Some authors have established the influence of the particle size and morphology of the BGs on this property, relating the increase in the surface area with a greater and faster release of alkaline species to the medium and therefore, with a higher increase into the medium pH (Waltimo et al., 2007). Others studies have established that the BGs production techniques lead to differences between them, the most active against bacteria being those performed by the sol–gel method (Balamurugan et al., 2008). In a recent study, we have extracted from literature a large database on the antibacterial properties of BGs and we have jointly analysed data using the neurofuzzy logic technique. Our results stated that the antibacterial properties of BGs are determined by the alkaline ions released, particularly calcium ions, and the increase of the pH of the medium (Echezarreta-López and Landin, 2013).

Quintero et al. have developed a new technique to produce "Laser spinning" glass nanofibers with different melt-derived compositions. Experimental conditions of laser-spinning method allow tailoring nanofibers of controlled composition, structure and geometry useful for the production of glass scaffolds. Moreover, the technique does not distort the glass structure of the precursor as demonstrated by magic angle spinning nuclear magnetic resonance (MAS-NMR) (Quintero et al., 2009a).

In this study, two laser spinning glass nanofibers have been produced with variations in the proportion of network modifiers. S18/12 nanofibers are elaborated with high silicon content whereas ICIE16 nanofibers incorporate high calcium content. Both types of nanofibers are amorphous (data not shown), fully dense with good consistency and flexibility. These properties facilitate their handling and the possibility of adapting them into complicated spaces.

Silicate glasses are considered inorganic polymers of silicon cross-linked by oxygen. Network connectivity (NC) is based on the relative number of network-forming oxide species which contribute in bridging or cross-linking silica tetrahedra, and network-modifying species that result in non-bridging oxygens (NBO) formation (Wallace et al., 1999; Watts et al., 2010).

Alkali and alkaline earth oxides replace bridging oxygens by NBO thus reducing network connectivity and opening up the glass structure (Varshneya, 1994; Elgayar et al., 2005).

The network connectivity of the S18/12 glass can be easily calculated assuming that each alkali ion creates one NBO and each alkaline earth cation creates two NBO (Varshneya, 1994), obtaining a NC = 3.38. On the other hand, in order to estimate the NC for the ICIE16 glass, the role of P_2O_5 in the silicate network must be taken into account (Elgayar et al., 2005; Grussaute et al., 2000; Aguiar et al., 2012). According to the results published by Elgayar et al. (2005), in the ICIE16 glass the proportion of orthophosphate and diphosphate are close to 75% and 25%, respectively. Then, the NC calculated using the relation published by Grussaute et al. (2000) is approximately NC = 2.12. The higher network connectivity has been related to a lower ion release and dissolution rate, together with a reduced bioactivity (Elgayar et al., 2005; Wallace et al., 1999; Martin et al., 2012). In fact, the bioactivity limits reported by Aguiar et al. (2012) as a function of the NC recalculated, taking into account the role of the phosphates, clearly classifying the ICIE16 glass as bioactive and the S18/12 as non-bioactive.

Additionally, variations in calcium and silicon ions during the *in vitro* bioactivity experiments (Fig. 2) are in agreement with the

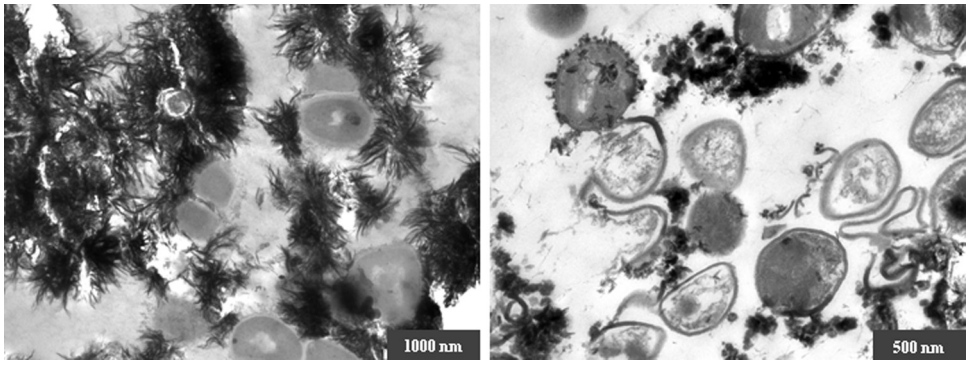

Fig. 10. TEM of ICIE16 after 4 days in the bacterial culture.

composition and structural differences between ICIE16 and S18/12 nanofibers making possible to classified S18/12 as bioinert and ICIE16 as bioactive nanofibers. The differences in ion released, between the nanofibers, does not have a significant effect on the evolution of pH in SBF. The pH of the medium increases during the first 24 h but remains the same after that time for both samples. This effect has been previously described by Vallet-Regi et al. (1999).

Several authors have described a critical period of 48 h in the biocompatibility experiments with bioactive glasses where an initial inhibition of cell proliferation takes place due to the adaptation of cells to the new growth medium (Mortazavi et al., 2010; Doostmohammadi et al., 2011) followed by the recovering in cell proliferation. The *in-vitro* biocompatibility studies, investigated through MTT tests (Fig. 3) show that bioactive glass nanofibers (ICIE16) promote lower percentages of cell viability in comparison with the bioinert glass nanofibers (S18/12) as a consequence of their bioactive nature and their release of ions in the medium. Despite of those differences, neither the ICIE16 nor the S18/12 glass nanofibers extracts at any concentration show high toxicity for fibroblast (BALB/3T3) cells at 24 h or 48 h, indicating high biocompatibility of samples.

The antibacterial properties of the two laser spinning glass nanofibers were studied in dynamic conditions using *S.aureus*. This common aerobic Gram positive bacteria is the main cause of the most of orthopaedic infections, decubitus ulcers and diabetic foot infections (Mortazavi et al., 2010). The antibacterial properties of BGs have been mainly associated to their chemical composition and dissolution properties. In particular, the release of alkaline ions into the environment and the associate increase in the pH of the medium has been established as the cause of the antibacterial effect of these biomaterials (Hu et al., 2009). However, studies with NaOH solutions promoting comparable variations in the pH of the medium did not show similar results suggesting the existence of additional reasons to justify the antibacterial properties of BGs. Several causes including the formation of oxygen radicals (Sawai et al., 1998) or the osmotic effect (Leppäranta et al., 2008) have been proposed. In a recent paper Echezarreta-López and Landin (2013) analysed from historical results the significant effect of an important number of different ions on the antibacterial properties of BGs and found that calcium release has a significant effect on this property, particularly on the Gram positive bacteria (Echezarreta-López and Landin, 2013). Despite variations among species, in general, calcium ions are lethal for Gram positive bacteria. This effect has been shown to be dose-dependent (Waltimo et al., 2007; Zhang et al., 2010). Those findings explain the differences between the antibacterial effects of the nanofibers (Fig. 4). ICIE16 nanofibers show a dose dependent bactericidal effect. The reduction in the growth index at a BG concentration of 75 mg mL^{-1} is important from the first day of incubation. Longer intervals are needed when the BGs concentration is lower.

Using identical experimental conditions, S18/12 nanofibers only allowed us to obtain a bacteriostatic effect at the highest BG concentrations and longest time. This unexpected bacteriostatic effect for a bioinert glass can favor some biomedical applications, using this material as the formation of bacterial biofilm on its surface can be avoid or reduced.

Our results agree with other authors reports (Munukka et al., 2008; Mortazavi et al., 2010) who have shown that glasses having calcium content of about 42.3% have higher antibacterial effect on aerobic bacteria than those containing 31.27% calcium content. Moreover, glasses with a lower CaO content (28.47%) have shown antibacterial activity when used at a BG concentration over 50 mg mL^{-1}. On this basis, the difference in CaO content between ICIE16 and S18/12, 33.1% and 8%, respectively, justifies their dissimilarity in antibacterial activity.

The significant increase of pH caused by ICIE16 nanofibers (Fig. 5) contributes to their antibacterial effect.

The ATR-FTIR analysis (Fig. 6) illustrates the structural differences among nanofibers and the modifications produced as a consequence of their incubation with bacteria culture. Spectra show, after the antibacterial studies, signals of partial dissolution for both the bioactive and the bioinert laser spinning nanofibers studied. Important reductions, particularly for ICIE16 nanofibers, in 980–1100 cm^{-1} bands indicate the modification of the structures to silica with a lower number of NBO as a consequence of their dissolution. These results are consistent with those discussed above.

The structural modifications of surface glass nanofibers, after the microbiological studies, were analyzed by SEM–EDX (Fig. 7). Semi-quantitative information on the chemical composition of the surface samples confirms the formation of a calcium phosphate layer on ICIE16 nanofibers as pointed out by the Ca/P ratio of this sample which has been related to the dissolution of bioactive glasses (Jones et al., 2001). The formation of a hydroxyapatite (Hap) layer on the surface constitutes the platform for different applications of several bioactive materials (Olmo et al., 2003). Hap is a calcium phosphate whose chemical composition is very similar to calcium phosphates in human bones. This characteristic makes the material biocompatible with living tissues. The properties of hydroxyapatite depend on the parameters, such as composition or crystallinity, and determine process, such as reabsorption and bioactivity.

SEM photomicrographs of the bacterial culture incubated with the nanofibers for 4 days show a thin layer on the surface of ICIE16 nanofibers and bacteria and not on the surface of S18/12 nanofibers (Fig. 8). Additionally, the TEM images show needle-like crystalline aggregates around the bacteria which contribute physically to their rupture and death. The physical action of needle crystals on bacteria has been also suggested by other authors to explain the antibacterial activity of bioactive glasses (Hu et al., 2009)

5. Conclusions

Two amorphous, dense and flexible glass nanofibers of different compositions have been successfully produced by a laser-spinning technique. Their differences in constitution and conformation determine their dissolution properties. Bioactivity studies allow the nanofibers with high proportion in SiO_2 (S18/12) to be classified as a bioinert glass and the nanofibers with high proportion of calcium (ICIE16) as a bioactive glass.

Cell viability tests indicated high biocompatibility of the laser spinning glass nanofibers. The release of ions from the nanofibers did not affect significantly the fibroblast cell viability. Results from the antibacterial activity study carried out using dynamic conditions revealed that the bioactive glass nanofibers show a dose-dependent bactericidal effect on *S. aureus* while the bioinert glass nanofibers show a bacteriostatic effect also dose-dependent. The antibacterial activity has been related to the release of alkaline ions, the increase of pH of the medium and also the formation of needle-like aggregates of calcium phosphate at the surface of the nanofibers which act as a physical mechanism against bacteria.

The antibacterial properties give an added value to the laser-spinning glass nanofibers for different biomedical applications, such as for treating or preventing surgery-associated infections. On this basis, consistent and flexible laser-spinning nanofibers are potentially useful to be used as bulk raw materials in composites, bone defects fillers or scaffolds (3D structures) for tissue engineering.

Conflict of interest

Authors declare no conflicts of interest.

Acknowledgements

Authors thank Ms. J. Menis for her help in the correction of the English version of the work and Dr. Helio Aguiar for his fruitful discussion. This work was partially supported by the POCTEP 0330IBEROMARE1P project, FEDER, UE and by Xunta de Galicia (CN2012/292). MMEL thanks the Galician Government (Xunta de Galicia, Spain) for financial support during the development of this work by IN.CI.TE. 2009–2013_Isabel Barreto Program.

References

Aguiar, H., Serra, J., González, P., 2012. A new quantitative method to predict the bioactive behavior of silicate glasses. J. Am. Ceram. Soc. 95, 2554–2561.
Allan, I., Newman, H., Wilson, M., 2001. Antibacterial activity of particulate Bioglass® against supra- and subgingival bacteria. Biomaterials 22, 1683–1687.
Balamurugan, A., Balossier, G., Laurent-Maquin, D., Pina, S., Rebelo, A., Faure, J., Ferreira, J., 2008. An in vitro biological and anti-bacterial study on a sol–gel derived silver-incorporated bioglass system. Dent. Mater. 24, 1343–1351.
Bellantone, M., Coleman, N.J., Hench, L.L., 2000. Bacteriostatic action of a novel four-component bioactive glass. J. Biomed. Mater. Res. 51, 484–490.
Boccaccini, A.R., Erol, M., Stark, W.J., Mohn, D., Hong, Z., Mano, J.F., 2010. Polymer/bioactive glass nanocomposites for biomedical applications: a review. Compos. Sci. Technol. 70, 1764–1776.
Bououdina, M., Rashdan, S., Bobet, J., Ichiyanagi, Y., 2013. Nanomaterials for biomedical applications: synthesis, characterization, and applications. J. Nanomater. 2013, 4.
Bressan, E., Sbricoli, L., Guazzo, R., Tocco, I., Roman, M., Vindigni, V., Stellini, E., Gardin, C., Ferroni, L., Sivolella, S., 2013. Nanostructured surfaces of dental implants. Int. J. Mol. Sci. 14, 1918–1931.
Chiara, G., Letizia, F., Lorenzo, F., Edoardo, S., Diego, S., Stefano, S., Eriberto, B., Barbara, Z., 2012. Nanostructured biomaterials for tissue engineered bone tissue reconstruction. Int. J. Mol. Sci. 13, 737–757.
Doostmohammadi, A., Monshi, A., Salehi, R., Fathi, M.H., Seyedjafari, E., Shafiee, A., Soleimani, M., 2011. Cytotoxicity evaluation of 63s bioactive glass and bone-derived hydroxyapatite particles using human bone-marrow stem cells. Biomed. Pap. Med. Fac. Univ. Palacky Olomouc Czech Repub. 155, 323–326.
Echezarreta-López, M., Landin, M., 2013. Using machine learning for improving knowledge on antibacterial effect of bioactive glass. Int. J. Pharm. 453, 641–647.
Efimov, A.M., Pogareva, V.G., 2006. IR absorption spectra of vitreous silica and silicate glasses: the nature of bands in the 1300 to 5000 cm^{-1} region. Chem. Geol. 229, 198–217.
Elgayar, I., Aliev, A., Boccaccini, A., Hill, R., 2005. Structural analysis of bioactive glasses. J. Non Cryst. Solids 351, 173–183.
Filgueiras, M.R., La Torre, G., Hench, L.L., 1993. Solution effects on the surface reactions of a bioactive glass. J. Biomed. Mater. Res. 27, 445–453.
Grussaute, H., Montagne, L., Palavit, G., Bernard, J.L., 2000. Phosphate speciation in Na_2O–CaO–P_2O_5–SiO_2 and Na_2O–TiO_2–P_2O_5–SiO_2 glasses. J. Non Cryst. Solids 263–264, 312–317.
Hench, L.L., Wilson, J., 1993. An Introduction to Bioceramics. World Scientific.
Hu, S., Chang, J., Liu, M., Ning, C., 2009. Study on antibacterial effect of 45S5 Bioglass®. J. Mater. Sci. Mater. Med. 20, 281–286.
Jones, J.R., 2013. Review of bioactive glass – from Hench to hybrids. Acta Biomater. 9, 4457–4486.
Jones, J.R., Sepulveda, P., Hench, L.L., 2001. Dose-dependent behavior of bioactive glass dissolution. J. Biomed. Mater. Res. 58, 720–726.
Khang, D., Carpenter, J., Chun, Y.W., Pareta, R., Webster, T.J., 2010. Nanotechnology for regenerative medicine. Biomed. Microdevices 12, 575–587.
Kokubo, T., 2008. Bioceramics and their Clinical Applications. Woodhead Pub. and Maney Pub.
Kokubo, T., Ito, S., Huang, Z., Hayashi, T., Sakka, S., Kitsugi, T., Yamamuro, T., 1990. Ca, P-rich layer formed on high-strength bioactive glass-ceramic A–W. J. Biomed. Mater. Res. 24, 331–343.
Leppäranta, O., Vaahtio, M., Peltola, T., Zhang, D., Hupa, L., Hupa, M., Ylänen, H., Salonen, J.I., Viljanen, M.K., Eerola, E., 2008. Antibacterial effect of bioactive glasses on clinically important anaerobic bacteria in vitro. J. Mater. Sci. Mater. Med. 19, 547–551.
Martin, R., Twyman, H.L., Rees, G.J., Barney, E.R., Moss, R.M., Smith, J.M., Hill, R.G., Cibin, G., Charpentier, T., Smith, M.E., 2012. An examination of the calcium and strontium site distribution in bioactive glasses through isomorphic neutron diffraction X-ray diffraction, EXAFS and multinuclear solid state NMR. J. Mater. Chem. 22, 22212–22223.
Mortazavi, V., Nahrkhalaji, M.M., Fathi, M., Mousavi, S., Esfahani, B.N., 2010. Antibacterial effects of sol–gel-derived bioactive glass nanoparticle on aerobic bacteria. J. Biomed. Mater. Res. Part A 94, 160–168.
Munukka, E., Leppäranta, O., Korkeamäki, M., Vaahtio, M., Peltola, T., Zhang, D., Hupa, L., Ylänen, H., Salonen, J.I., Viljanen, M.K., 2008. Bactericidal effects of bioactive glasses on clinically important aerobic bacteria. J. Mater. Sci. Mater. Med. 19, 27–32.
Olmo, N., Martin, A.I., Salinas, A.J., Turnay, J., Vallet-Regi, M., Lizarbe, M.A., 2003. Bioactive sol–gel glasses with and without a hydroxycarbonate apatite layer as substrates for osteoblast cell adhesion and proliferation. Biomaterials 24, 3383–3393.
Parratt, K., Yao, N., 2013. Nanostructured biomaterials and their applications. Nanomaterials 3, 242–271.
Quintero, F., Pou, J., Comesaña, R., Lusquiños, F., Riveiro, A., Mann, A.B., Hill, R.G., Wu, Z.Y., Jones, J.R., 2009a. Laser spinning of bioactive glass nanofibers. Adv. Funct. Mater. 19, 3084–3090.
Quintero, F., Dieste, O., Pou, J., Lusquiños, F., Riveiro, A., 2009b. On the conditions to produce micro- and nanofibres by laser spinning. J. Phys. D 42, 65501.
Santhana Raj, L., Hing, H., Omar, B., Hamidah, Z., Aida Suhana, R., Nor Asiha, C., Vimala, B., Paramsarvaran, S., Sumarni, G., Hanjeet, K., 2007. Rapid method for transmission electron microscope study of *Staphylococcus aureus* ATCC 25923. Ann. Microsc. 2007 7, 102–108.
Saravanakumar, B., Rajkumar, M., Rajendran, V., 2011. Synthesis and characterisation of nanobioactive glass for biomedical applications. Mater. Lett. 65, 31–34.
Sato, M., Webster, T.J., 2004. Nanobiotechnology: implications for the future of nanotechnology in orthopedic applications. Expert Rev. Med. Devic. 1, 105–114.
Sawai, J., Shoji, S., Igarashi, H., Hashimoto, A., Kokugan, T., Shimizu, M., Kojima, H., 1998. Hydrogen peroxide as an antibacterial factor in zinc oxide powder slurry. J. Ferment. Bioeng. 86, 521–522.
Serra, J., González, P., Liste, S., Serra, C., Chiussi, S., León, B., Pérez-Amor, M., Ylänen, H., Hupa, M., 2003. FTIR and XPS studies of bioactive silica based glasses. J. Non Cryst. Solids 332, 20–27.
Stoor, P., Söderling, E., Salonen, J.I., 1998. Antibacterial effects of a bioactive glass paste on oral microorganisms. Acta Odontol. 56, 161–165.
Vallet-Regi, M., Salinas, A., Roman, J., Gil, M., 1999. Effect of magnesium content on the in vitro bioactivity of CaO–MgO–SiO_2–P_2O_5 sol–gel glasses. J. Mater. Chem. 9, 515–518.
Varshneya, A.K., 1994. Fundamentals of Inorganic Glasses. Gulf Professional Publishing.
Wallace, K., Hill, R., Pembroke, J., Brown, C., Hatton, P., 1999. Influence of sodium oxide content on bioactive glass properties. J. Mater. Sci. Mater. Med. 10, 697–701.
Waltimo, T., Brunner, T., Vollenweider, M., Stark, W., Zehnder, M., 2007. Antimicrobial effect of nanometric bioactive glass 45S5. J. Dent. Res. 86, 754.
Watts, S., Hill, R., O'Donnell, M., Law, R., 2010. Influence of magnesia on the structure and properties of bioactive glasses. J. Non Cryst. Solids 356, 517–524.
Zhang, D., Leppäranta, O., Munukka, E., Ylänen, H., Viljanen, M.K., Eerola, E., Hupa, M., Hupa, L., 2010. Antibacterial effects and dissolution behavior of six bioactive glasses. J. Biomed. Mater. Res. Part A 93, 475–483.